353. Failure analysis of destructive coils

R. Kačianauskas [1,a], A. Kačeniauskas[2,b], E. Stupak[1,c], S. Balevičius[3,d], N. Žurauskienė[3,e] and J. Novickij[4,f]
[1,2,4]Vilnius Gediminas Technical University, Saulėtekio 11, Vilnius, Lithuania
[3]Semiconductor Physics Institute, A. Goštauto 11, Vilnius, Lithuania
E-mail: [a]*rimantas.kacianauskas@fm.vtu.lt*, [b]*arnka@fm.vtu.lt*, [c]*Eugenius.Stupak@fm.vtu.lt*, [d]*sbal@pfi.lt*, [e]*zurausk@pfi.lt*, [f]*jurij.novickij@el.vtu.lt*

(Received 17 April 2008; accepted 13 June 2008)

Abstract. The failure of the destructive pulsed power coils has been investigated. The destructive coil is the key element of the laboratory system which generates half-period abrupt magnetic field pulses with the amplitudes up to 45 T. The transient coupled non-linear magneto-mechanical model has been applied for finite element simulations. The mechanical behavior and operation threshold of the coil have been examined. It has been found that operation threshold of the coil with relatively thin cylindrical reinforcement could be characterized by the opening of the plastic hinge and estimated numerically. Good agreement with experimental results has been observed.

Keywords: failure analysis, destructive coils, pulsed high magnetic fields, coupled magneto-mechanical model, finite element method.

Introduction

A pulsed power coil for generation of high magnetic fields can be considered as the main component of complex mechatronic systems such as electromagnetic launchers, rail guns and other electromagnetic actuators [1-3]. Control and measurement of the parameters of magnetic field pulses is a complicated process since their irregular waveforms can contain abrupt rise and decay stages [3]. Experimental investigation of destructive coils and their failure analysis is technically complex and costly. Therefore numerical simulation presents an attractive alternative to handle this multi-physical problem.

In this work, we suggest using destructive coils for generation of high magnetic field pulses with decay times significantly shorter than the pulse rise time and duration. In order to generate such pulses, it is necessary to induce fast discharge of electric energy accumulated inside the coil [1]. This can be realized by means of fast "short-circuiting" of the coil windings in the following way. An increase in the current through the coil induces a simultaneous increase in the magnetic and mechanical forces. This results in higher stress on the coil windings and subsequent deformation of its structure. At certain current thresholds the mechanical forces induce structural displacements of the windings in the radial direction. As a result, the windings are short-circuited and magnetic field energy is transformed to discharge arcs and heating of the coil. This process is sufficiently fast to enable generation of abrupt decays in the magnetic pulse that can be used for testing the operational speeds of the magnetic sensors. The instant in time at which the coil loses its functionality and the discharge process starts is termed as "coil operation threshold". It can be predicted numerically on the basis of mechanical considerations. A coupled non-linear transient magneto-mechanical analysis based on Maxwell's equations and the non-linear equilibrium equation can be used for this purpose.

Maxwell's partial differential equations represent a fundamental unification of electric and magnetic fields in predicting electromagnetic phenomena. For the numerical simulation of electromagnetic phenomena, three basic discretization techniques, namely, finite difference [4], finite element [5], and finite volume methods [6] may be used. The finite element method (FEM) for unstructured grids is well adapted to complex geometries and to local mesh refinements. The solution of 3D eddy current problems using Maxwell's equations and magnetic vector potential was presented in [7]. Numerical analysis and design of electromagnetic coils was performed in [8].

The progress in the simulation of particular fields stimulated the development of numerical methods for multi-physical phenomena including coupled fields [9]. Available numerical analyses are strongly dependent on the application. The reduction of anodic connector electrical losses was investigated using a coupled thermo-electro-mechanical FEM model [10]. Magnetic field investigations were coupled with linear mechanical analysis in [11]. Strong coupling of magnetic and mechanical analysis was investigated by Delaere et al [12]. The newest achievements have made a strong impact on the development of general purpose FEM codes, such as ANSYS [13] containing multi-physical utilities and

electromagnetic fields for coupled analysis. The major investigations have been, and continue to be, focused on improving intelligent modeling strategies.

Mathematical Model

In the following transient magnetic analysis, for a given current density $\boldsymbol{J}$, the temporal and spatial evolution of the magnetic flux density $\boldsymbol{B}$ is described by Maxwell equations [7, 13]:

$$\nabla \times \boldsymbol{H} = \boldsymbol{J}, \quad (1)$$

$$\nabla \cdot \boldsymbol{B} = 0, \quad (2)$$

$$\nabla \times \boldsymbol{E} = -\frac{\partial \boldsymbol{B}}{\partial t}, \quad (3)$$

where $\boldsymbol{H}$ is the magnetic field intensity vector and $\boldsymbol{E}$ is the electric field intensity vector. Neglecting permanent magnets, the constitutive relation is:

$$\boldsymbol{H} = [\upsilon]\boldsymbol{B}, \quad (4)$$

where $[\upsilon]$ is the reluctivity matrix, which is the inverse of magnetic permeability $[\mu]$. In ferromagnetic regions, the constitutive relation (Eq. 4) is represented by a non-linear curve. Reflecting magnetic properties of the media, Maxwell Eq. 1-3 can be solved employing the potential field approach [7].

High magnetic fields generate very large electromagnetic forces that act on a stranded coil during the pulse operation. The resulting Lorenz forces can be computed from the magnetic flux density:

$$\boldsymbol{F}^{\mathrm{EM}} = \boldsymbol{J} \times \boldsymbol{B}, \quad (5)$$

Mechanical behavior of the coil is governed by a time-dependent non-linear equilibrium equation written in terms of time-dependent displacements $\boldsymbol{u}(t)$:

$$\nabla_{\mathrm{S}} \cdot ([\boldsymbol{D}(\boldsymbol{u})]\nabla_{\mathrm{S}}^{T}\boldsymbol{u}) = \boldsymbol{F}^{\mathrm{EM}}, \quad (6)$$

where ∇_{S} is the divergence operator of the stress tensor and $[\boldsymbol{D}]$ is a fourth-rank non-linear material constant tensor. It reflects the development of plastic deformations with assumed von Misses plasticity and hardening. The force vector $\boldsymbol{F}^{\mathrm{EM}}(t)$ represents the electromagnetic loads.

The numerical model for performing the coupled magneto-mechanical analysis is based on the finite element software ANSYS [13]. The structural problem is weakly coupled to the magnetic problem by the electro-magnetic force vector $\boldsymbol{F}^{\mathrm{EM}}$. In the work presented here, the magneto-mechanical analysis is performed in the directly coupled fashion by considering all advantages of the multi-physical approach.

Description of the Problem

The destructive coil used to investigate fast magnetic sensors was developed by Novickij et al. [3]. The laboratory device that generates half-period sinus-shaped magnetic field pulses of 0.15-2 ms duration and with amplitudes up to 45 T in a 12 mm diameter bore, was investigated numerically. The coil was fabricated using multi-layer technology and included 6 layers of copper wire with 18 turns in each layer. During the winding process, each layer was insulated with the epoxy-glass fiber composite. The inside diameter of the coil is d = 12 mm and the outside diameter of the coil is D = 32 mm, while the length is l = 30 mm. The coil was placed in a steel cylinder to reinforce the construction. The inside diameter of the cylinder was 40 mm, the outside diameter - 50 mm and the length - 40 mm. The coil windings were separated from the inner surface of the steel cylinder by a 4 mm thick epoxy-glass fiber composite layer. The fabricated coil was mounted inside the 11 mm thick steel container to insure safety during experiments.

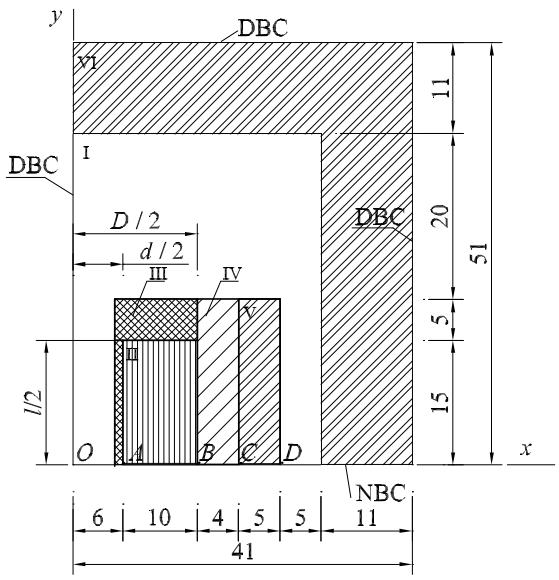

Fig. 1. The geometry of solution domain and boundary conditions

The axisymmetric formulation of the coupled problem (Eq. 1-6) is investigated in the analysis of the coil. Due to its axial symmetry, only a quarter of the coil section is considered in the 2D solution domain, which is defined for the OXY plane. The geometry of a quarter section of the device is depicted in Fig. 1. In this axisymmetric case, only the z component of the potential vector $\boldsymbol{A}$ and the two displacement components u_x and u_y are not equal to zero. Standard boundary conditions are prescribed for the boundaries of the solution domain. The natural Newman boundary conditions (NBC) for the magnetic potential are specified for the OX axis. The Dirichlet boundary

conditions (DBC) are specified on the rotating symmetry axis OY and on the external part of the solution domain. The components of the normal displacements are fixed for the symmetry axis in the mechanical analysis. The magnetic load is created by the source current density [13].

Finally, the unbounded solution domain is replaced by a rectangular box having the dimensions of 41×51 mm. It consists of six different regions: air (region I), windings of the coil (region II), epoxy-textolite (region III), epoxy-glass separation layer (region IV), cylinder reinforcement (region V), and steel container (region VI). The magnetic properties of these regions are predefined by using the relative magnetic permeability $\mu = 1$ for all materials with the exception of the steel, the non-linear magnetic properties of which are defined by the material property curve [14]. Non-linear behavior of the magnetic field of the steel is observed when the magnetic flux density B reaches a value equal to 1.5 T.

The structural material properties are defined as follows. The steel used to make the hollow cylinder and the container were assumed to be an elastic-perfectly-plastic linear material with elasticity modulus of E_a = 200 GPa and yield limit σ_{0a} = 300 MPa. The epoxy-glass separation layer, due to its high strength limit σ_{0c} = 3400 MPa, is assumed to be purely elastic, with effective elasticity modulus of E_c = 10 GPa [15]. The coil winding area, which is as a layered copper-epoxy-glass composite, was simulated by assuming that it is a homogeneous elastic perfectly-plastic material, with effective elasticity modulus of E_c = 90 GPa, Poisson's ratio - 0.34, and effective yield stress limit - σ_{0c} = 400 MPa.

Results and Discussions

The numerical model was validated by performing transient magnetic analysis described by Eq. 1-3. The first experiment was performed at room temperature, T = 295 K. The time variation of the experimentally measured current (Iexp) is plotted in Fig. 2a. The experimental data was processed and incorporated in the numerical magnetic analysis in terms of a source current density ***J***. The sinus-shaped source current with an amplitude of 4.2 kA generates a magnetic field, which reaches a maximum value of B = 16 T at the central point of the coil. A quantitative comparison of the numerical results (Bnum) with the experimental measurements (Bexp) at the central point of the coil is shown in Fig. 2b. Numerical analysis predicted the pulse of the magnetic field very accurately: the error did not exceed 1.3 %. A second experiment was performed at a temperature of T = 77 K. The coil was cooled by liquid nitrogen. The experimentally measured current (IexpT) is also plotted in Fig. 2a. The resulting numerical solution (BnumT) is compared with the results of the experimental measurements (BexpT) in Fig. 2b. The results are in fairly good agreement with the error of only 1-2.4%.

The most important issue in the numerical analysis is, however, the prediction of the operation threshold of the coil. The finite element simulation of the destructive coil is based on the transient coupled magneto-mechanical analysis described by the mathematical model Eq. 1-6. Numerical simulations and experimental tests were performed in the same manner as in the previous example. The main difference may be characterized by higher values of input current. The actual

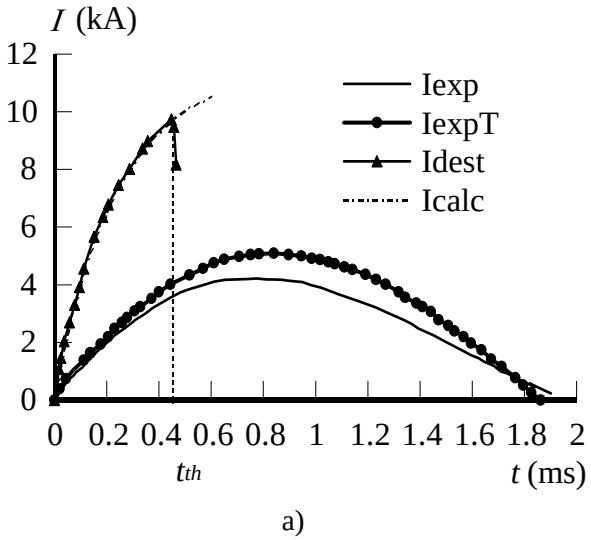

a)

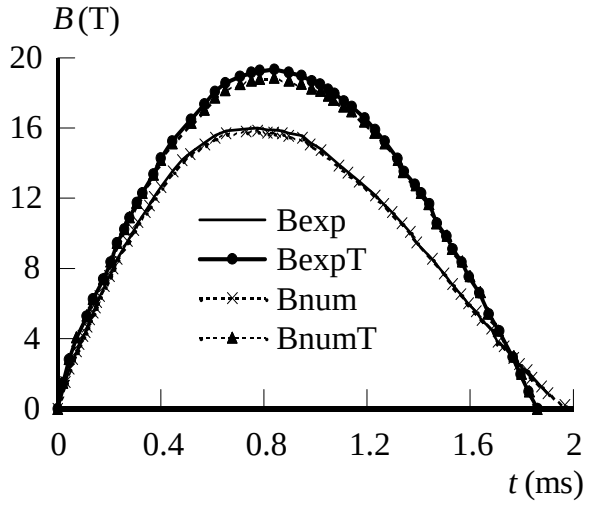

a

Fig. 2. The time evolution of the source current (a) and flux density (b) in the central point of the coil: numerical results and experimental measurements

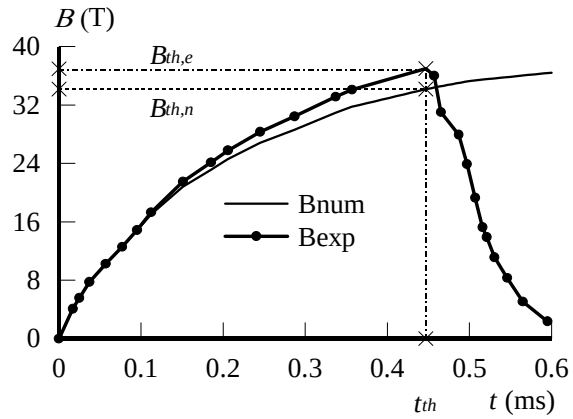

Fig. 3. Time evolution of field magnetic flux density at the central point of the destructed coil

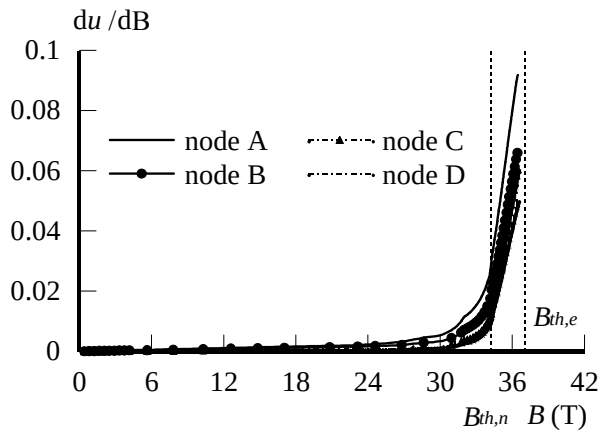

Fig. 4. Variation of radial displacement derivatives d*u*/d*B* against magnetic flux density at characteristic points of mid-plane

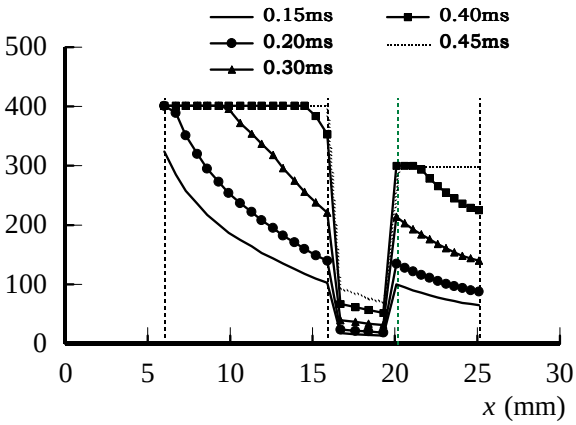

Fig. 5. Radial variation of Mises stress in central section at different time instants

thresholds are obtained by experimental testing. The variation of the experimentally measured current (Idest) is plotted in Fig. 2a. It proves that the experimental coil operation threshold was reached at time t_{th} = 0.45 ms. The experimental curve was extrapolated up to 0.06 ms for modeling purposes.

The quality of the numerical analysis is examined by comparing it to experimental results. A comparison of the experimental and numerical results for the time variation of the magnetic field flux density is presented in Fig. 3. It proves that the experimental threshold value $B_{th,e}$ is equal to 37 T, while simulation results yield a numerical threshold of $B_{th,n}$ = 35 T. The difference in the two curves, which indicates a 5.4% difference in the threshold values, may be explained by the influence of different factors, for example, local imperfections, change in the geometry, thermal influence, etc. The operation threshold may be recovered on the basis of numerical results of mechanical analysis. It was found that the variation in displacements may be used as an indicator of the mechanical behavior and used to evaluate the operating threshold of the structure. Variations in the radial displacement derivatives d*u*/d*B* at characteristic points A, B, C and D located in mid-plane (Fig. 1) versus magnetic field flux density are presented in Fig. 4. Examination of these results indicates that the displacement variation contains almost constant deformation rates and transition regions located between 32 and 35 T. The end of transition region corresponds to the numerically obtained operation threshold $B_{th,n}$ = 35 T.

The reason for the occurrence of a mechanical threshold may be explained by the results of elastic-plastic stress analysis. Radial variations in the stress at different time instances are presented in Fig. 5 and illustrate stress evolution during magnetic loading. By increasing the magnetic field, the stress peak occurring in the internal boundary of the wire windings reaches the yield limit and causes the wire to move outwards. The operation threshold is characterized by the yielding of outer cylinder reinforcement, which has a limit of σ_{0a} = 300 MPa. It is indicated by the presence of a spreading plastic zone in the entire mid-plane and may be characterized as a circular plastic hinge. This phenomenon is quite well-known in the mechanics of thin-walled structures.

Conclusions

Within the frame of the current investigations, the transient coupled magneto-mechanical finite element model was applied for numerical analysis. The performance of the magnetic part, as well as the discretization model, were verified by experimental measurements of the magnetic flux density. The operation threshold of a destructive coil was evaluated by using mechanical finite element analysis. Characteristic points in the time history of the displacements indicate that the destructive coil has an operation threshold. It was found that the operation threshold corresponds to the yield point of the mid-plane section and behaves like a circular plastic hinge in the cylinder reinforcement. The numerically obtained operation threshold value was in good agreement with experimental measurements.

References

[1] **Herlach F.** Physica B Vol. 319 (2002), p. 321-329.

[2] **Witte H. , Jones H.** Physica B Vol. 346-347 (2004), p. 663-667.

[3] **Novickij J., Stankevič V., Balevičius S., Žurauskienė N., Cimmperman P. , Kačianauskas R., Stupak E., Kačeniauskas A., Löffler M. J.** Solid State Phenomena Vol. 113 (2006), p. 459-464.

[4] **Yee K. S.** IEEE Transactions on Antennas and Propagation Vol. 14(4) (1966), p. 302-307.

[5] **Zienkiewicz O. C., Arlett P. L., Bahrani A. K.** The Engineer Vol. 224 (1967), p. 547-550.

[6] **Mohammadian A. H., Shankar V., Hall W.** Computer Physics Communications Vol. 68(1-3) (1991), p. 175-196.

[7] **Bíró O., Preis K.** IEEE Transactions on Magnetics Vol. 25(4) (1989), p. 3145-3159.

[8] **Mohammed O. A., Garcia L. F.** IEEE Transactions on Magnetics Vol. 25(5) (1989), p. 3575-3577.

[9] **Hameyer K., Driesen J., De Gersem H., Belmans R.** IEEE Transactions on Magnetics, Vol. 35(3) (1999), p. 1618-1621.

[10] **Richard D., Fafard M., Lacroix R., Cléry P., Maltais Y.** Finite Elements in Analysis and Design, Vol. 37(4) (2001), p. 287-304.

[11] **Bouillault F., Buffa A., Maday Y., Rapetti F.** Computer Methods in Applied Mechanics and Engineering Vol. 191(23-24) (2002), p. 2587-2610.

[12] **Delaere K., Heylen W., Hameyer K., Belmans R.** Journal of Magnetism and Magnetic Materials Vol. 226-230(2) (2001), p. 1226-1228.

[13] **ANSYS** Theory Reference, 8th edition (SAS IP INC. 2003).

[14] **Balevičius S., Žurauskienė N., Novickij J., Kačeniauskas A., Kačianauskas R., Stupak E.** Journal of Information Technology and Control, Vol. 3(8) (2003), p. 54-82.

[15] **Berthelot J. M.** *Composite Materials. Mechanical Behavior and Structural Analysis* (Springer-Verlag, New York 1999).